

# The Formation of Structural Imperfections in Semiconductor Silicon



# The Formation of Structural Imperfections in Semiconductor Silicon

By

V. I. Talanin and I. E. Talanin

Cambridge  
Scholars  
Publishing



The Formation of Structural Imperfections in Semiconductor Silicon

By V. I. Talanin and I. E. Talanin

This book first published 2018

Cambridge Scholars Publishing

Lady Stephenson Library, Newcastle upon Tyne, NE6 2PA, UK

British Library Cataloguing in Publication Data

A catalogue record for this book is available from the British Library

Copyright © 2018 by V. I. Talanin and I. E. Talanin

All rights for this book reserved. No part of this book may be reproduced, stored in a retrieval system, or transmitted, in any form or by any means, electronic, mechanical, photocopying, recording or otherwise, without the prior permission of the copyright owner.

ISBN (10): 1-5275-0635-5

ISBN (13): 978-1-5275-0635-0

# CONTENTS

|   |     |
|---|-----|
| Preface .....   | vii |
| Chapter One.....  | 1   |
| Growth of Dislocation-Free Silicon Single Crystals from Melt and Defect Formation   |     |
| 1.1. Features of the growth of dislocation-free single crystals of silicon by the methods of floating zone melting and the Czochralski..... | 2   |
| 1.2. Defect structure arising in the process of growth of dislocation-free single crystals of silicon .....                                 | 8   |
| 1.3. Experimental researches of the impurity kinetics of the formation of grown-in microdefects.....  | 21  |
| 1.4. Researches of the transformation of grown-in microdefects during various technological influences.....                                 | 47  |
| Chapter Two .....   | 64  |
| Physical Modeling of Defect Formation Processes in Dislocation-Free Single Crystals of Silicon  |     |
| 2.1. Early physical models of the formation of grown-in microdefects .....  | 65  |
| 2.2. Recombination-diffusion model for the formation of grown-in microdefects .....   | 68  |
| 2.3. Model of the dynamics of point defects.....  | 74  |
| 2.4. Heterogeneous (two-stage) model of grown-in microdefect formation .....  | 86  |
| 2.5. About various approaches to solving the problem of defect formation in silicon .....   | 90  |
| Chapter Three .....   | 94  |
| Physical Basis of a Heterogeneous (Two-Stage) Model of Grown-In Microdefect Formation   |     |
| 3.1. Recombination of intrinsic point defects in silicon and the classical theory of nucleation .....                                       | 94  |
| 3.2. About the accordance of process of the high-temperature precipitation and the classical theory of nucleation.....                      | 99  |

|   |     |
|---|-----|
| Chapter Four .....  | 106 |
| High-Temperature Precipitation of Impurity in Dislocation-Free Silicon Single Crystals  |     |
| 4.1. Basic concepts of the microscopic theory of impurity kinetics in semiconductors .....  | 108 |
| 4.2. Model of dissociative diffusion-migration of impurities .....  | 116 |
| 4.3. Kinetics of the high-temperature precipitation process in dislocation-free silicon single crystals.....  | 138 |
| 4.4. Complex formation in semiconductor silicon within the framework of Vlasov's model for solids.....  | 147 |
| 4.5. Kinetic model of growth and coalescence of precipitates of oxygen and carbon during the cooling of silicon crystal after growing .....   | 154 |
| Chapter Five .....  | 170 |
| The Formation of Microvoids and Interstitial Dislocation Loops during Crystal Cooling After Growing   |     |
| 5.1. Modeling of the processes of formation of microvoids and interstitial dislocation loops within the framework of point defects dynamic model .....  | 171 |
| 5.2. The vacancy condensation model .....   | 181 |
| 5.3. Kinetic model of formation and growth of interstitial dislocation loops.....   | 188 |
| Chapter Six .....   | 198 |
| General Approach to the Engineering of Defects in Semiconductor Silicon   |     |
| 6.1. Necessary conditions for the engineering of defects during the crystal growth .....  | 199 |
| 6.2. Structure of the diffusion model .....   | 205 |
| 6.3. Diffusion model of the formation of grown-in microdefects as applied to the description of defect formation in heat-treated silicon single crystals. Thermal donors and thermal acceptors .... | 210 |
| 6.4. The technique of virtual research of defect structure .....  | 219 |
| 6.5. Use of information technologies for analysis and management of defect structure of initial single crystals and devices based on them.....  | 224 |
| Summary .....   | 235 |
| References .....  | 239 |
| Supplement.....   | 268 |

## PREFACE

*We are to admit no more causes of natural things than such as are both true and sufficient to explain their appearances*

—Isaac Newton (25.XII.1642 – 20.III.1727)

*Philosophiæ Naturalis Principia Mathematica*, 1726

Over the past few decades, our knowledge of the solid state nature has increased significantly. At the same time the scope of application of crystalline solids in various fields of technology has greatly expanded. The increasing technological demands stimulate the rapid development of a relatively young area of modern natural science – solid state chemistry, the main tasks of which are as follows: synthesis of solids, research of their physical and chemical properties, reactions thereof, and ultimately creation of materials with predetermined properties.

All real solids (monocrystalline and polycrystalline) contain structural defects. Structural defects are violations of the periodicity of the spatial arrangement of atoms. The appearance of defects in crystals is inevitable, since they are formed in the process of a single crystal growth. The impact of defects on the physical properties of crystals is extremely diverse. It is determined by the nature of the binding forces in crystals, their energy structure (metals, semiconductors or dielectrics). If the fundamental physical properties of a substance are determined by its chemical composition and perfect structure, the introduction or change in the concentration of defects can change these properties, as well as impart new optical, electronic, mechanical and other characteristics to the substance. Creating a fairly complete picture of the nature and behavior of various defects is a prerequisite for a scientific approach to control structurally sensitive properties and processes in solids. Therefore, the most informative path to study any solid crystals is to consider their structure, formation, and properties as a joint and inseparable overall problem.

Semiconductor silicon occupies a completely unique position of all the variety of solids. Semiconductor (or electronic) silicon is considered to be basis of the electronic industry at present and in the foreseeable future. Discrete instruments and microelectronic integrated circuit are made of silicon. Requirements for the quality of silicon single crystals are

constantly increasing due to transition to production of large and very large scale integrated circuits and associated increase in the single crystal diameter and the degree of microelectronic circuit integration. Microelectronics requires to grow single crystals, which are completely dislocation-free, with a uniform distribution of doping and background impurities, with controlled and limited content of intrinsic structural point defects. Such stringent requirements stimulate intensive research into the nature of defect formation and improvement of techniques for obtaining modern dislocation-free silicon single crystals.

Requirements for the quality of modern microelectronic devices have made silicon the purest material in the world. Silicon single crystals are obtained by means of Czochralski method and floating zone melting method. Both methods ensure the production of the initial silicon with the total content of residual impurities  $10^{11} \dots 10^{12} \text{ cm}^{-3}$ . The specific resistance of single crystals obtained by the floating zone melting method can reach up to  $100 \text{ k}\Omega \cdot \text{cm}$ , they show a large diffusion length of charge carriers and a low oxygen content. Such hyperpure crystals are an excellent research laboratory to study the general principles of defect formation. In addition, semiconductor silicon is the most suitable model for this kind of research as one of the most studied and used by humankind materials.

The growth of dislocation-free silicon single crystals by the Czochralski and floating zone melting methods is accompanied by the formation of structural imperfections known as grown-in microdefects. The formation of grown-in microdefects is mainly caused by intrinsic point defects (vacancies and interstitial silicon atoms) and impurity atoms of oxygen and carbon. The problem of controlling the nature, content, size, and nature of distribution of defects present in the dislocation-free silicon single crystal is primarily related to the development of effective methods for influencing the state of the ensemble of interacting point defects in the grown ingot. Advances in control of the point defects ensemble state ultimately determine the success of the quality management of electronic devices. Therefore, studying of formation and growth causes of various grown-in microdefects under different growing conditions of dislocation-free silicon single crystals is of high applied significance.

The problem of grown-in microdefects formation is both of technological (defect structure control in the process of crystal growing), and of fundamental scientific importance because its solution makes it possible to describe the physics of defect formation in hyperpure dislocation-free silicon single crystals. At the same time, it is impossible to solve the technological aspect of the problem of grown-in microdefects formation without understanding the physics of grown-in microdefects



formation process in dislocation-free silicon single crystals. This requires knowledge and correct physical model of grown-in microdefects formation and transformation to be adequately applied. This model is built using comprehensive experimental researches of dislocation-free silicon single crystals obtained by the Czochralski and floating zone melting methods at varying thermal conditions in the course of crystal growth.

The quantitative model of defect formation in dislocation-free silicon single crystal should be only developed based on such a qualitative mechanism, which adequately reflects a real crystal structure. The quantitative model of grown-in microdefects formation, in its turn, allows to simulate and to obtain dislocation-free silicon single crystals with a predetermined defect structure and to control it during further process effects. The quantitative model of grown-in microdefect formation should give an answer to the fundamental question of solid state physics, which consists in describing the kinetics of the grown crystal defect structure during its cooling. The development of such a model for the most perfect silicon crystals can serve as a basis for considering similar problems for other dislocation-free single crystals. The patterns of defect formation in dislocation-free single crystals are common, thus, silicon can be an example of structure analysis for all semiconductor and metallic dislocation-free single crystals.

Most publications about the defect structure of dislocation-free silicon single crystals are more or less associated with the investigation of point defects interaction in the course of dislocation-free silicon single crystals growth, elucidating the nature of the grown-in microdefects, and revealing the relationship between thermal conditions of crystal growth and formation of structural imperfections. A lot of international conferences carried out in recent years were devoted to these issues. However, up to the present time, there are no enough focused reviews in the scientific literature which would analyze the problems of grown-in microdefects growth and transformation from a common viewpoint. This monograph, to some extent, can compensate and eliminate these deficiencies.

The book considers experimental results of studying the nature of grown-in microdefects. The main attention is focused on the experimental and theoretical investigation of the point defects interaction in silicon, the elucidation of physical and chemical nature of grown-in microdefects, their transformation in the course of dislocation-free silicon single crystals growth, as well as the analysis of existing physical and mathematical models of the grown-in microdefects formation. The monograph is the result of a critical comprehension of a large number of original experimental and theoretical works presented in various scientific journals.

In a number of cases, there are significant differences in the experimental data and their interpretation. This difference is mainly due to the fact that there are two ways to solve the problem of defect formation in dislocation-free silicon single crystals. Followers of the first approach assume that there is rapid recombination of intrinsic point defects (IPDs) under the crystallization temperature and suggest that simulation of IPD dynamics in silicon may contribute to a quantitative understanding of the grown-in microdefects formation process and to their spatial distribution optimization inside the crystal. This approach assumes the dominant role of IPDs in the structural imperfection formation and leads to negation of the impurity involvement in this process. Followers of the second approach governed by the obtained experimental results deny the fact of IPD recombination in silicon at high temperatures and suggest that the problem of defect formation in dislocation-free silicon single crystals can be solved by creating a physical model based on the known experimental results to the fullest extent possible. In this case, it is assumed that defect formation in silicon is based on the interaction ‘impurity – intrinsic point defect’. The main goal of this monograph is an attempt to understand these contradictions and to present a real picture of defect formation in dislocation-free silicon single crystals.

The monograph consists of six chapters. The first chapter considers features of (1) dislocation-free silicon single crystals growth by floating zone melting and Czochralski methods; (2) modern ideas about the defect structure arising in the process of their growth; (3) a review of experimental studies on the impurity kinetics of grown-in microdefects formation; (4) results of studies on various process-caused transformations of grown-in microdefects.

The second chapter is devoted to the analysis of physical simulation models of defect formation processes in semiconductor silicon. In particular, we considered early physical models of grown-in microdefects formation (equilibrium and nonequilibrium interstitial models, drop, vacancy and vacancy-interstitial models). Special attention was paid to the recombination-diffusion model proposed by V.V. Voronkov which can be considered as a symbiosis of all the pre-existing models. We considered a strong approximation of a mathematical model of intrinsic point defects dynamics developed on the basis of a recombination-diffusion model in detail. The main provisions of the heterogeneous (two-stage) model, as well as the origins of various approaches to solving the problem of defect formation in semiconductor silicon are briefly discussed.

The third chapter deals with critical issues for understanding the heterogeneous (two-stage) model. It is explained why the interaction

‘impurity – intrinsic point defect’ has an advantage over the IPD recombination processes in the course of crystal growth under high temperatures. It is shown how to reconcile the high-temperature precipitation process with the classical theory provisions related to the second phase particles nucleation.

The fourth chapter considers two new approaches to solve the problem of theoretical description of defect formation processes in the course of crystal growth: the high-temperature impurity precipitation model and the complex-formation model based on Vlasov equation solution for imperfect crystals. Firstly, we described the high-temperature impurity precipitation model in the course of crystal growth. We considered basic concepts of the microscopic theory of impurity kinetics in semiconductors and chose the model of dissociative diffusion-migration of impurities as a model for complex formation in the course of silicon single-crystal growth. We discussed the kinetics of high-temperature impurity precipitation process in dislocation-free silicon single crystals. As an alternative, we considered the problem of complex formation in semiconductor silicon in accordance with A. A. Vlasov model for solids. It was discovered that two nucleation theories of second phase particles, which are based on various approaches (classical nucleation theory and Vlasov model for solids), lead to identical results. A kinetic model of oxygen and carbon precipitates growth and coalescence during the grown silicon crystal cooling is presented.

The fifth chapter discusses the formation of microvoids and interstitial dislocation loops in the course of crystal growth. Formation processes of microvoids and interstitial dislocation loops within the framework of the point defect dynamics model were simulated. A vacancy-condensation model, as well as a kinetic model of interstitial dislocation loops formation and growth were proposed.

A general approach to the engineering of defects in silicon is given in the sixth chapter. The necessary conditions for defect engineering during crystal growth are briefly discussed. We considered the diffusion model structure of grown-in microdefects formation and transformation and its application to describe the defect formation in heat-treated silicon single crystals. The technique of defect structure virtual research is given. It is considered as an assistant tool to use modern information technologies in order to analyze and control defect structure of initial single-crystals and instruments made of such crystals. Presented is a computation algorithm for semiconductor silicon defect structure used in the development of software products.

The content of this book mostly reflects the authors’ research area, thus, some issues related to point defect interaction were not included and

others were considered briefly and concisely due to limited volume of the book. Despite this, the authors do hope that this monograph can be useful both for professionals and students, as well as can be used as a reference material.

It should be noted that all chapters of this book are written by both authors and each of them has the same copyright to the material presented in the book. There is no conflict of interests between the authors.

## CHAPTER ONE

# GROWTH OF DISLOCATION-FREE SILICON SINGLE CRYSTALS FROM MELT AND DEFECT FORMATION

*When we meet a fact which contradicts a prevailing theory, we must accept the fact and abandon the theory, even when the theory is supported by great names and generally accepted*

—Claude Bernard (12.VII.1813 – 10.II.1878)

*An Introduction to the Study of Experimental Medicine, 1865*

The development of electronics is based on the development of microelectronics as the leading sub-sector of world electronic production; because microelectronic technologies are now the pinnacle of engineering in the field of high technologies and they determine the achievable technical level of the country's industrial potential. On the one hand modern rates of microelectronics development are associated with advances in the field of semiconductor technology, and on the other hand they lead to increasingly stringent requirements for the semiconductor industry. These requirements can be met by means of different technologies and materials, but due to the needs of mass production and relative cheapness of the material, the monocrystalline silicon grown by the Czochralski method is the main material in the microelectronic industry. Economic reasons led to a steady increase of grown single crystals in the diameter and length, as far as more crystals can be cut from a larger diameter wafer (the square dependence of area on diameter). Modern growth units in combination with developed growing modes and precision control systems allow growing high-quality single crystals with a diameter of up to 350 mm on an industrial scale and mastering the production of single crystals with a diameter of 450 mm. A greater output of suitable products is possible only in case of high axial and radial homogeneity in impurity composition and low content of grown-in microdefects in growing dislocation-free silicon single crystals.

## **1.1. Features of dislocation-free silicon single crystals growth by floating zone melting and the Czochralski methods**

Two main methods of growing silicon single crystals are used in the industry: extraction from quartz crucibles (Czochralski method) and floating zone melting [1, 2]. To obtain silicon single crystals by the Czochralski method (hereinafter referred to as CZ-Si) polycrystalline silicon is placed in high purity quartz crucible heated to the melting point of silicon ( $\sim 1683 \dots 1685 \text{ K}$ ). A seed of a certain section and a given orientation cut from a single crystal is lowered into the melt and a part of the seed is melted slightly by raising the temperature. After this, the heater temperature is slowly lowered until crystallization on the seed begins. At this point, the seed is lifted, and the single crystal is drawn out of the melt. The diameter of the grown single crystal is regulated by the temperature of the heater, the rate of lifting the rod, the conditions for removing the heat of crystallization, and other parameters. To obtain silicon single crystals with a given type of conductivity and resistivity a doping impurity (boron, phosphorus, antimony, arsenic, aluminum, etc.) is introduced into the crucible with a charge or into the melt in pure form or in the form of ligature. The growing process demands suitable conditions for the dopant to be uniformly distributed throughout the volume of the single crystal. It is extremely difficult to create a strictly symmetrical thermal field; crystal or crucible (or both) rotate to equalize the temperature field, which makes it possible to grow symmetrical single crystals even at large asymmetric temperature gradients.

Due to the thermal field asymmetry so-called ‘screw thread’ is observed on the cylindrical surface of single crystals grown with rotation: Crystal growth rate increases when passing the cold area of the melt and more impurities are captured at this point. In hotter area the growth rate decreases. Such periodic microscopic fluctuations in the crystal growth rate cause the phenomenon of ‘remelting’, which is responsible for the banded distribution of impurities in the crystal longitudinal section and leads to the formation of grown-in microdefects in the swirl distribution along the crystal cross-section [3]. In addition to the ‘screw thread’, one can see annular irregularities on the surface of a single-crystal related to the fluctuations of the melt level, its temperature, rod movement velocity, etc.

The main shortcoming of CZ-Si crystal growth is the increased content of carbon (up to  $5 \cdot 10^{16} \text{ cm}^{-3}$  and over) and oxygen (up to  $18 \cdot 10^{18} \text{ cm}^{-3}$ ), as

well as other impurities contained in the quartz crucible from which the ingot is drawn.

Unlike CZ-Si, silicon single crystals obtained by the floating zone method (hereinafter referred to as FZ-Si) are distinguished by a very low content of such background impurities as oxygen and carbon. The concentration of these impurities in some crystals may be below the sensitivity level of optical methods (less than  $5 \cdot 10^{15} \text{ cm}^{-3}$ ).

To obtain FZ-Si a polycrystalline rod shall be vertically fixed in the unit clamps. The molten zone is created by induction heating, and this zone is retained by surface tension forces. The smaller the zone height, the larger ingot diameter it can occupy. A single-crystal seed is strengthened in the lower clamp and a molten drop is created at the end of the rod. Then the seed is moved upward and introduced into the melt. After seeding, the seed, along with the single crystal growing on it, is moved downward (or the inductor is lifted up). Repeated zone movement due to evaporation and difference in impurity distribution coefficients in liquid and solid states can lead to a very high degree of silicon purification. To produce silicon single crystals with a given level of resistivity, volatile compounds of the dopant (phosphine, diborane, arsine, etc.) are introduced into the unit chamber or polycrystalline rods are used preliminarily doped in the course of hydrogen reduction or monosilane decomposition. The pedestal growth is a variation of the floating zone melting method. In this case, the seed is installed in the upper clamp and the molten zone is created at the upper end of the rod.

Dislocation-free single-crystals make more than 95 % of the silicon single crystals obtained. Dislocation-free single crystals are grown by the Dash method [4]. This method consists in high-rate growing of a long thin monocrystalline neck with a diameter less or equal to the seed diameter after seeding. Once a section free from dislocations is found on a certain neck section, a conical and then a cylindrical part of a single crystal of a given diameter may be grown.

Theoretical analysis and practical growing of silicon single crystals in any crystallographic direction allow us to conclude that the growth of these crystals is accomplished by the appearance and development of planes  $\{111\}$ . In this case, growth begins with the formation of a two-dimensional nucleus. While the two-dimensional nucleus is developed in a tangential direction at a low rate because of the boundary large curvature a number of other nuclei are formed on its surface. This process continues until the curvature radius decrease in normal direction leads to the growth rate decrease. By this time, the curvature radius is increased in tangential direction and growth in this direction quickly outstrips growth in normal

direction. Once the face is overgrown with the layer formed, the process resumes.

Thermal stresses arising in a growing crystal as a result of curvature of isothermal surfaces, one of which is the crystallization surface, can lead to plastic deformation and structural defect formation. The number and distribution of structural defects and associated changes in electrical and physical properties of single crystals are largely determined by the magnitude and distribution of thermal stresses defined by thermal growth environment. The thermal growth environment can be defined by the crystallization front shape. For example, it is possible to obtain a simple relation, determined by the macroscopic growth front shape of a single crystal as a function of the drawing rate. It is necessary to preserve the condition  $V_p = V_g$  ( $V_p$  – drawing rate;  $V_g$  – the rate of the heat flow across the interface or the growth rate of the crystal) to prevent liquid detachment from the crystal. This rate can be determined by Fick's equations. Thus, for a planar interface

$$\frac{\partial^2 T}{\partial z^2} = \frac{\partial T}{\partial t} = \frac{\partial T}{\partial z} \frac{\partial z}{\partial t} = \frac{\partial T}{\partial z} V_z. \quad (1.1)$$

Hence, heat flow rate through a flat surface equals

$$V_z = \frac{\partial^2 T / \partial z^2}{\partial T / \partial z}. \quad (1.2)$$

For a spherical interface

$$\frac{\partial^2 T}{\partial r^2} + \frac{2}{r} \frac{\partial T}{\partial r} = \frac{\partial T}{\partial t} = \frac{\partial T}{\partial r} \frac{\partial r}{\partial t} = \frac{\partial T}{\partial r} V_r \quad (1.3)$$

whence

$$V_r = \frac{\partial^2 T / \partial r^2}{\partial T / \partial r} + \frac{2}{r}. \quad (1.4)$$

Thus, heat flow through a spherical surface  $V_r = V_z + 2/r$ , where  $T$  is a temperature;  $r$  is a distance from the interface. Hence, if  $V_r = V_p$ , then  $V_p - V_z = 2/r$ . If  $V_p = V_z$  a flat interface is maintained; if  $V_p > V_z$ , a concave crystallization front arises, and if  $V_p < V_z$  – a convex crystallization front arises. Type of the crystallization front has a significant influence on the temperature distribution at the interface. Curvature of the crystallization front is the main parameter used to estimate changes in thermal growth environment.



Radial temperature gradients arising in the crystal and determining thermal stress magnitude are proportional to the tangent of the isothermal surface curvature angle and the axial temperature gradients:

$$\frac{\partial T}{\partial r} = \frac{\partial T}{\partial a} \operatorname{tg} \theta, \quad (1.5)$$

where  $\frac{\partial T}{\partial r}$  and  $\frac{\partial T}{\partial a}$  are the radial and axial temperature gradients respectively;  $\operatorname{tg} \theta$  is the slope of the curve to the isothermal surface.

As the rate of the zone passage increases, the curvature of the crystallization front decreases. Decrease of the crystallization front curvature and increase of the passage rate can be explained by the following reasons:

- Firstly, as the passage rate increases, the amount of evolved crystallization heat increases;
- Secondly, the melting power should be increased to maintain a stable zone, which leads to more intensive melt mixing.

Both factors contribute to a more uniform temperature distribution in the zone area. An increase in the passage rate also leads to a decrease in the axial temperature gradient. Consequently, as the passage rate increases, the value of both parameters decreases on the right-hand side of Eq. (1.5), which corresponds to a decrease in the radial temperature gradient and the associated thermal stresses and structural defects.

As the crystal grows, the conditions of the heat transfer through the crystallization front and the melting front should be changed along the zone transfer path. So, as the zone moves, heat removal through the crystallization front should increase, and heat removal through the melting front should decrease. This should lead to increase of the axial temperature gradients in the growing crystal and increase of the crystallization front curvature. Since silicon thermal conductivity coefficient is a finite value, increase of the axial temperature gradient in the course of zone movement along the ingot should mainly appear when crystals are grown at lower rates of the zone passage.

The dependence of the axial temperature gradient on the rate of the zone shift was expressed in [5] by the empirical formula for the first time for small-scale crystals of FZ-Si (up to 30 mm):

$$\frac{dT}{dx} = 10 + (x - 16)^2 \exp(-61.2V_g - 0.28), \quad (1.6)$$

where  $x$  is the distance from the crystallization front to a certain cross section, cm. An analytical determination of the two-dimensional

temperature field was proposed in [6, 7] for large-scale CZ-Si crystals (over 100 mm). According to this technique, the temperature field is set as follows:

$$\frac{1}{T} = \frac{1}{T_m} + \frac{G_a x}{T_m^2} \quad (1.7)$$

where  $T_m$  is the crystallization temperature,  $x$  is the distance from the crystallization front,  $G_a$  is the axial temperature gradient. The temperature field is set both axial-wise and along the surface; a field along the crystal's surface to axial-wise field ratio changes incrementally. It was shown in [8] that the joint usage of formulas (1.6) and (1.7) to calculate the defect formation shows similar results. Similar results obtained by two methods prove the absence of fundamental differences between them, their interchangeability and the possibility of their application to crystals of any diameters [8].

The most typical shapes of the crystallization front for CZ-Si and FZ-Si are shown in Fig.1.1.

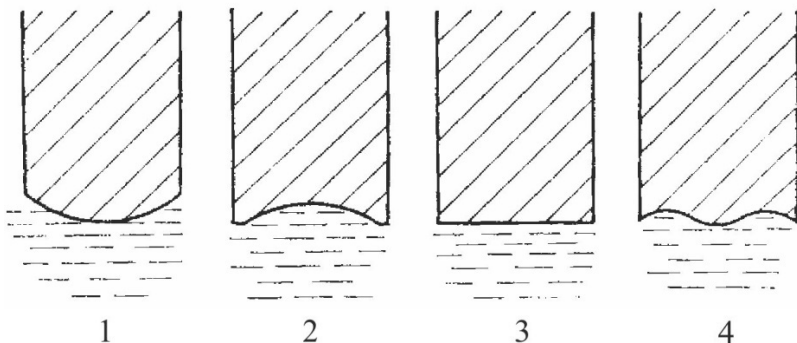


Fig. 1.1. The shape of the crystallization front during the growth of silicon single crystals: (1) convex; (2) concave; (3) flat; (4) undulating.

In fact, the crystallization front is not limited by a smooth surface, but by a stepped surface. Flat areas of different lengths can be often observed on the crystallization front, depending on the growth direction. In addition, macro- and microdepressions, protrusions, etc. may be formed in some cases. The shape of the crystallization front depends on the growth modes, and if silicon single crystals are grown in the [111] direction, a plane molecular smooth surface appears along the surface of the crystal-liquid contact with the rounded sections. In contrast to the flat growth front

(when  $V_p = V_g$ ), as a rule being a stepped surface with a low step height, the formed face turns out to be mirror-smooth. If the crystallization front is convex, then the face is formed on a rise (deep in the liquid). If the front is concave towards the crystal, the face is formed on the peripheral part of the circle. It is established that this face coincides with the crystallographic face (111) of the silicon lattice. In addition to the horizontal face (111), lateral lower and upper faces (111) also appear on the crystallization front. When growing in directions different from [111], for example, [100], only the side faces come out to the crystallization front. It should be noted that the crystallization front surface of dislocation-free and dislocation silicon single crystals differs significantly. This difference is manifested primarily in the sharp increase of the face protrusion area (111) on the crystallization front in the course of the growth of dislocation-free silicon single crystals.

The channel inhomogeneity was discovered long ago and used to be the main reason causing an inhomogeneous distribution of impurities along the cross-section of silicon single crystals grown in the [111] direction. Channel inhomogeneity arises because of the face effect appearance under certain conditions causing the crystallization front face formation (111). For this crystal face is grown in a relatively more super-cooled melt than its surrounding, then impurity concentration in the crystal face area is higher. Although the channels are detected both when the crystallization front is concave (to the seed) and almost flat, they are formed mainly at the convex towards the melt crystallization front.

When single crystals are grown with a wave-type crystallization front, we observe a core-type and tubular-type channels. These channels appear in points of the face protrusion (111) on the crystallization front. Increase in size of a flat area of the crystallization front results in expanding a channel's width. A curvature decrease of the crystallization front leads to a wider central (core-type) channel and decreasing of a tubular-type channel diameter. A sharp change of the crystallization front can lead to the channel disappearance. The crystallization front is flat near the channel.

The main reason for the channel inhomogeneity formation is the growth of single crystal by the two-dimensional nucleation (coupled with the single crystal rotation and drawing in the direction [111]), which leads to increased super-cooling in the face protrusion (111) on the crystallization front area.

The number and distribution of structural imperfections largely depend on the magnitude and distribution of thermal stresses, determined by the thermal growth conditions. Since the crystallization front shape with sufficient accuracy reflects the isotherm corresponding to the silicon melting temperature, this shape identification and study allow us to

characterize a single crystal thermal growth conditions. The macroscopic shape of the crystallization front, in its turn, is determined by the crystal growth rate. Indeed, the growth rate increase causes the crystallization front curvature decrease and the axial temperature gradient decrease. The most technically simple way is to control the growth rate, while accurate measurements of the temperature gradient meet certain difficulties [9, 10].

## **1.2. Defect structure arising in the process of dislocation-free silicon single crystals growth**

According to the generally accepted geometric (dimensional) classification [11], structural defects in crystals are subdivided into:

- point (zero-dimensional): vacancies, interstitial atoms (intrinsic and impurity atoms);
- linear (one-dimensional): dislocations of various types; flat (two-dimensional): stacking faults, interphase and intraphase interfaces;
- three-dimensional: voids, precipitates.

Structural imperfections called ‘grown-in microdefects’ are formed during high-temperature growth and subsequent cooling of high-purity dislocation-free silicon single crystals. Since the dislocation-free crystals are supersaturated by point defects (vacancies, self-interstitials, impurity atoms) in the cooling process, the formation of grown-in microdefects is due to the processes of IPD and impurity aggregation. The impossibility of complete material purification (presence of residual or background impurities) and occurrence of IPDs (vacancies and silicon self-interstitials) at the crystallization temperature even in special undoped high-purity silicon single crystals obtained by the floating zone method result in complex interaction processes and subsequent decomposition of the oversaturated solid solution of point defects during the crystal cooling [12]. Structural imperfections (micro-precipitates, dislocation loops, microvoids) formed in such processes are grown-in microdefects. Thus, pursuant to a contemporary view, the term microdefects is taken to involve any local disturbances of the lattice periodic behavior measuring from several tens of angstroms to several micrometers. They form an intermediate class between point and other types of structural defects and also are aggregates of IPDs and impurities [13]. In turn, microdefects formed during silicon processing were called the ‘post-growth’ microdefects.

Information about the presence of etch pits in dislocation-free silicon single crystals for the first time appeared in the second half of the 1960s

[14]. On the (111) plane, these pits have the shape of regular triangles with sides directed along [110]. Unlike ordinary dislocation etch pits, they have a flat bottom, and therefore were called as empty etch pits in those works. The [15] describes the arrangement of empty pits in a single crystal body and the influence of a number of factors on their appearance for the first time in detail, and assumes the vacancy origin of these defects.

De Kock began to classify the empty etch pits, having called them clusters. He introduced two types of clusters depending on the etch pit size: A-clusters (A-microdefects) and B-clusters (B-microdefects) [15, 16]. Taking into account that the macro-pattern of empty etch pit distribution along a single crystal cross-section in most cases resembles vortices, the authors of [17, 18] called these microdefects as swirl defects. It was shown that microdefects are located along impurity growth bands, which, in turn, reflect the shape of the crystallization front, determined by the thermal conditions of growth [19, 20]. The minimum spacing between the spiral bands corresponds to the ratio of the crystal growth rate to its rotation speed. As the crystal growth rate decreases, the deflection of the microdefect bands increases, which is explained by increase of the temperature gradient radial component [20]. Density of microdefects in the band was found to be higher than at the periphery of the center of the crystal. The authors [20] state that this may be caused by the fact that the temperature gradient radial component in the center of the crystal is always higher than at the periphery at the observed crystallization surface curvature. Both types of defects may be observed in the crystal body. Herewith, the distribution of B-microdefects (small etch pits) is often superimposed on the distribution of A-microdefects (large etch pits). The maximum size of B-microdefects is observed in areas where there are no A-microdefects. A- and B-microdefects can be found in the central part and are usually absent at the side crystal surface. Furthermore, B-microdefects are located closer to the single crystal surface than A-microdefects. The crystal surface can serve as a drain for intrinsic point defects, so, as a rule, the near-surface areas, contain few microdefects. The average concentration of A-microdefects in the crystal body is  $\sim 10^6 \dots 10^7 \text{ cm}^{-3}$ , while average concentration of B-microdefects is  $\sim 10^9 \dots 10^{10} \text{ cm}^{-3}$  [21, 22]. Experiments on crystal quenching have shown that B-microdefects are formed first [16, 19].

It should be noted that until the end of the 1970s grown-in microdefects were investigated mainly in small-sized FZ-Si crystals (26...30 mm in diameter). In silicon single crystals of 30 mm in diameter banded distribution of typical A-microdefects were found to be observed at the crystal growth rates  $V_g = 1.0 \dots 3.5 \text{ mm/min}$ , uniform distribution

thereof at  $V_{\text{cr}} < 1.0$  mm/min; while banded distribution of B-microdefects was found to be observed at  $V_{\text{cr}} \leq 4.5$  mm/min [12]. Fig. 1.2 shows typical banded distribution of A-microdefects along the crystal cross-section, and Fig. 1.3 shows swirl distribution of B-microdefects in the (111) plane [23].

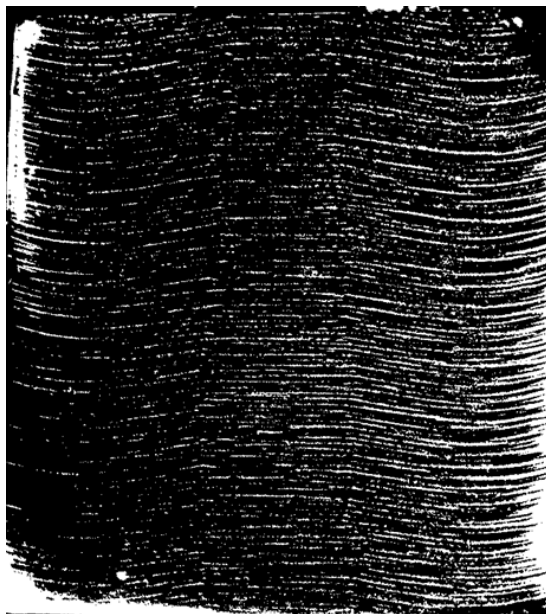


Fig. 1.2. Banded distribution of A-microdefects in the plane [112], selective etching, crystal diameter 30 mm



Fig. 1.3. Swirl distribution of B-microdefects in the plane [111], selective etching, crystal diameter 30 mm

As the size of the A-microdefects increases to a certain limit (ca. 40  $\mu\text{m}$  at  $v_g = 1.0$  mm/min) [19] dislocations arise in silicon single crystals [19, 24, 25]. With the help of transmission electron microscopy (TEM), it was shown that A-microdefects could act as sources of dislocation nucleation, which, pursuant to the authors [26], is due to the Frank-Read mechanism action, under the influence of compressive stresses in the center of the crystal resulting from the combined effect of radial and axial temperature gradients. Appearance of dislocations is seriously affected not only by the dimensions, but also by relative disposition of microdefects, and by distances between them, since their growth and interaction take place at temperatures corresponding to the plasticity zone [20].

Abe conducted an analysis of the impurity effect on microdefect formation and showed that the formation of A- and B-microdefects is enhanced by crystal doping with carbon and is impeded by oxygen [3]. The formation of microdefects is suppressed by doping with impurities of large covalent radii, for example, antimony. Banded distribution of A- and B-microdefects is associated with the sites of their nucleation. When the crystal is grown, temperature fluctuations occur due to crystal rotation and melt convection. As a result, microdefects grow following the crystal type of growth and stopping [3, 27, 28]. Periodic changes in the crystal growth rate cause respective periodic changes in the impurity concentration, in particular, carbon. It was shown [28] that the local maxima of the concentration of microdefects (bands of A- and B-microdefects) coincide

with areas of high phosphorus concentration. Based on the fact that banded distribution of A- and B-microdefects is also observed in phosphorus-free silicon and taking into account the similarity of phosphorus and carbon distribution [28, 29], the authors of [18, 30-32] concluded that the microdefects should be formed with the participation of carbon atoms. Foll et al. determined that concentration of microdefects increases as carbon content increases [18]. On this basis, it was concluded that the banded distribution of microdefects indicates a heterogeneous nature of their nucleation and its dependence upon periodic changes in crystal growth rate [18]. The critical crystal growth rate at which the remelting phenomenon is suppressed, which contributes to the nonuniform distribution of impurities in the crystal was calculated theoretically in [33] (for floating zone melting method  $\sim 5.3$  mm/min). This value is in good agreement with the experimental results [34], under which disappearance of B-microdefects occurs. Based on these results, it can be concluded that temperature fluctuations and the presence of impurities (especially carbon [18, 32, 35, 36] and oxygen [37-40]) are the main factors responsible for the formation of A- and B-microdefects.

At a certain growth rate, it is possible to achieve the absence of large microdefects. For example, disappearance of A- and B-microdefects in FZ-Si crystals occurs at very low cooling rates, which is achieved by growing crystals at a growth rate of  $V_g \leq 0.2$  mm/min [41]. At such low growth and cooling rates, the concentration of point defects as a result of their diffusion to the crystal surface decreases below a certain critical value necessary for the formation of microdefects [41]. In this case, the amplitude of impurity bands also decreases, which is related to the diffusion process in the solid state and respective composition homogenization. With an increase in crystal growth rate up to 4.0...4.2 mm/min A-microdefects are not detected, and at a growth rate of more than 4.5 mm/min B-microdefects are not detected as well [42-45]. Based on these experimental data, the authors of [15, 41] proposed methods for obtaining dislocation-free silicon single crystals without microdefects. However, obtaining homogeneous and defect-free silicon single crystals at very low growth rates is characterized by low process productivity, which is a very significant drawback [20]. In addition, in this case, it is difficult to maintain the dislocation-free mode, since dislocations may be generated during an unforeseen decrease in the crystal growth rate [19].

Until 1975, it was believed that A- and B-microdefects are vacancy clusters generated during the growing crystal cooling on various vacancy-oxygen complexes. However, TEM-studies of dislocation-free silicon single crystals revealed that A-microdefects are individual dislocation



loops of 1...5  $\mu\text{m}$  size or clusters of such interstitial-type loops [26, 27, 42]. These investigations did not provide any direct study of B-microdefects in a 'pure' form in theory. Only pre-decoration of microdefects allowed to make an assumption about their interstitial origin [27]. Further detailed TEM-studies confirmed this hypothesis [45].

When crystals are grown at sufficiently high rates (above 4.5 mm/min for FZ-Si crystals), a new type of microdefects was observed as uniform distribution and could be identified as dim regions after preferential etching and decoration [46]. These defects were classified as C- or D-microdefects depending on their macrodistribution images [46]. Both types were visualized as the regions with uniform defect distribution of high density and, according to the authors of the paper [46], differed from each other by distribution geometry in these regions. The uniform D-microdefects distribution is focused in the form of a 'channel' in the central part of the crystal (Fig. 1.4a). At the same time, C-microdefects were observed as rings or circles of irregular shape, located at the most extensively cooled parts of the crystal. Later de Kock confirmed the existence of identical grown-in microdefects in small-scale CZ-Si crystals (50 mm in diameter), which were observed after selective etching [47, 48].

It should be noted that in [46] defects were named D-microdefects which were observed after selective etching in a uniform distribution in the form of a channel in the center of a 30 mm diameter FZ-Si crystal grown at  $V_g \leq 6.0$  mm/min. With the help of TEM, the physical nature of D-microdefects (the sign of defect-induced lattice imperfection) discovered in [46], was studied in detail [21, 49]. It was shown that D-microdefects (and C-microdefects) formed in crystals grown at growth rates above 4.5 mm/min  $\leq V_g \leq 6.0$  mm/min are interstitial by nature, i.e., they cause compression deformation in the crystal.

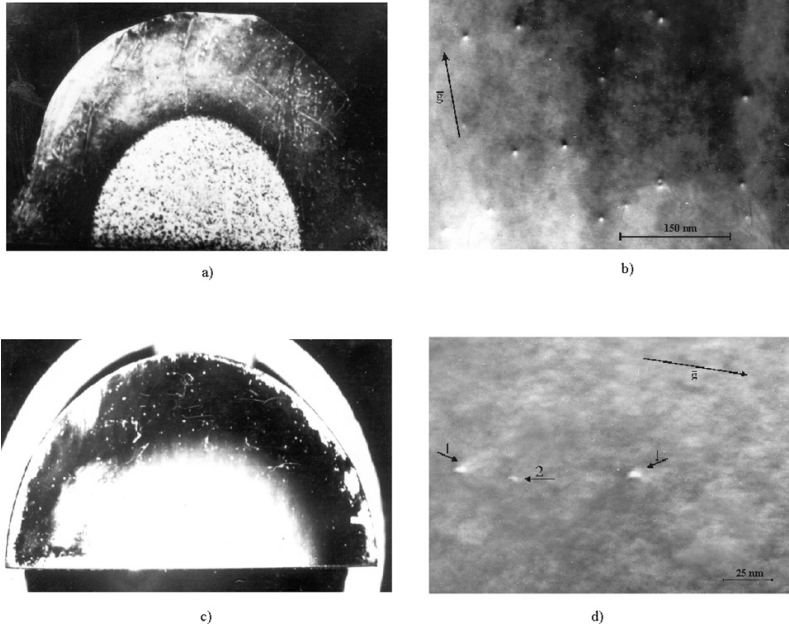


Fig. 1.4. D-microdefects and (I+V)-microdefects of FZ-Si crystals (crystal diameter 30 mm):

(a) D-microdefects, selective etching, plane (111); (b) D-microdefects, TEM, dark field,  $\bar{g} = (\bar{2}20), s = 0$ ; (c) (I+V)-microdefects, selective etching, plane (111); (d) (I+V)-microdefects ((1) V-defects; (2) I-defects), TEM, dark field,  $\bar{g} = (\bar{2}20), s = 0$ .

Four years after the paper [46] Roksnoer and van den Boom also investigated uniform defects distribution in the center of a 30 mm diameter FZ-Si crystal grown at  $V_g > 6.0$  mm/min [50]. On the basis of X-ray topography results coupled with subsequent copper decoration, it was assumed that D-microdefects are vacancy-type. This erroneous assumption had a great influence on subsequent theoretical studies of defect formation in silicon, since it formed the basis for the recombination-diffusion model of the grown-in microdefects formation (Voronkov model) [6]. Later it was shown that under these conditions (I+V)-microdefects are formed (Fig. 1.4c) [13]. (I+V)-microdefects are coexisting defects of the vacancy (V) and interstitial (I) type (Fig. 1.4d) [13, 51, 52].

It should be noted once again that all the above data refer to silicon single crystals with a diameter of 28...30 mm. However, the known data allow us to state that as the crystal diameter is increased; the growth rates are reduced resulting in the disappearance of A- and B-microdefects and the appearance of D-microdefects. For example, in [3] it is pointed out that in silicon single crystals with a diameter of 42 mm, D-microdefects are formed at a growth rate of 4.0 mm/min, while the formation of A- and B-microdefects in larger single crystals with a diameter of  $\sim 125$  mm is

suppressed at a growth rate  $V_g > 2.5$  mm/min. These results can be explained by a decrease in the axial temperature gradient in the crystal, which occurs when the diameter of the grown crystal is increased. Therefore, defect formation in large-scale crystals is of great interest, since the modern electronic industry is characterized by an increasing tendency to use silicon single crystals of large diameters [53-55]. However, as shown in [53], defects ensemble in large-diameter crystals does not undergo serious changes, and, probably, mechanisms of defect formation are generally uniform for single crystals of any diameter. It should only be taken into account that as the diameters increase, the differences in the temperature growth conditions of such crystals become effective.

In the process of CZ-Si single crystal growth temperature growth conditions and content of impurities significantly differ from those applied to obtain silicon by the floating zone melting method. Carbon concentration in these crystals is one order of magnitude higher, and oxygen concentration is one or two orders of magnitude higher and makes  $\sim 10^{16} \dots 10^{18} \text{ cm}^{-3}$ . Furthermore, the Czochralski method is characterized by a lower cooling rate.

Etching patterns of A-, B-, and D-microdefects found in CZ-Si were identical to those found in FZ-Si crystals [47, 48, 50]. Banded distribution of A- and B-microdefects is observed in undoped or slightly doped monocrystals with a diameter of 50 mm grown at  $V_g \leq 1.0$  mm/min.

Furthermore, at  $V_g \sim 1.0$  mm/min A- and B-microdefects are formed in concentrations comparable to their concentration in silicon single crystals

obtained by the floating zone melting method. At  $V_g \geq 2.0$  mm/min the formation of A- and B-microdefects is completely suppressed, and the presence of uniformly distributed D-microdefects is observed [56]. The distribution of A-microdefects depends on the amplitude of fluctuations in the crystal microscopic growth rate [57]. If the microscopic growth rate varies significantly, the banded distribution of microdefects takes place, otherwise the uniform distribution takes place. The critical growth rate at

which the A-microdefects disappear is  $\sim 2.0$  mm/min [47]. This value decreases with the crystal diameter increase and with the axial temperature gradient decrease. As known, the axial temperature gradient near the crystallization front decreases as the growth rate increases and as the crystal diameter increases [54]. The value of 2.0 mm/min obtained by the authors of [47] is in good agreement with the calculated growth rate required to suppress the remelting phenomenon ( $\sim 2.7$  mm/min) [33] caused by temperature instability due to thermal convection.

Due to the high content of impurities in CZ-Si single crystals, the defect ensemble is also strongly dependent on residual and dopant impurities. For example, doping with acceptor impurities almost suppresses the formation of B- and D-microdefects, donor doping eliminates A-microdefects [58, 59]. Oxygen is present in CZ-Si single crystals in fairly high concentrations (up to  $\sim 2 \cdot 10^{18}$  cm<sup>-3</sup>), it penetrates into silicon from a quartz crucible [15, 49, 60, 61]. Such a high content of oxygen determines its significant influence on such single crystals' parameters. Oxygen precipitation has a significant effect on the crystal electrical and mechanical properties [62-64], and it is in close interrelation with the defect structure of silicon single crystals [65-67]. In addition, the authors of [68-71] indicate that carbon should also be as important as oxygen in CZ-Si crystals, and that concentrations of B- and D-microdefects depend upon the carbon concentration [47, 57, 68, 72]. Based on these results, as well as on the identity of main types of microdefects in FZ-Si and CZ-Si crystals, and taking into account the strong dependence of microdefects in FZ-Si crystals on carbon impurity [18], it was concluded that carbon should play the key role in microdefects formation in CZ-Si crystals [73, 74].

In earlier papers devoted to CZ-Si crystals [47, 48], D-microdefects were identified based on the nature of their distribution, and for this reason, according to [46], they were for some time referred to as C- and D-microdefects. In addition, further research was conducted using various detection techniques, which led to a disparity in the names of the same defects. An attempt was made in [75] to classify microdefects in crystals grown by the Czochralski method on the basis of X-ray topography results coupled with selective decoration. D-microdefects of FZ-Si crystals were named as A'-microdefects in this paper. The authors of [75, 76] showed banded distribution of A'-microdefects. A type of defects called  $\alpha$ -defects [75] was also identified. The dimensions of the etching patterns and the density of the A'- and  $\alpha$ -microdefects were identical, but taking into account uniform distribution of  $\alpha$ -defects in contrast to A'-defects, the authors of [75] identified them as a separate type of defects. Herewith,

theoretical results [6] showed that  $\alpha$ -microdefects are formed at the boundary of interstitial- and vacancy-type growth, while A'-microdefects are formed in the course of vacancy-type growth [75]. The technique used by the authors could not specify the type of detected defects (interstitial or vacancy), and therefore  $\alpha$ -microdefects were treated as defects of 'unknown nature' [65, 66, 75]. The situation with the nature of microdefects of the A'-type was also unclear. Repeatedly pointing out the identity of A'-microdefects with D-microdefects of FZ-Si and postulating the interstitial origin of A'-microdefects, the authors of [76-78] found the main differences between these two types of microdefects in the nature of their distribution: banded for A'-microdefects and uniform for D-microdefects. Subsequently, still pointing out the identity of both types of defects, but assuming the vacancy origin of D-microdefects [50], the A'-microdefects were regarded as defects of the vacancy origin and identified as

*'oxygen microprecipitates formed as a result of joint oxygen-vacancy agglomeration' [40, 65, 79-81].*

New types of grown-in microdefects are observed in large-scale CZ-Si crystals (diameter over 100 mm). In particular, the formation of so-called oxidation-induced stacking faults (OSF-ring) after thermal oxidation of annular distribution along the cross-section perpendicular to the growth axis is the most typical at present [82, 83]. Stacking faults arise around plate-like oxygen precipitates, and bulk density of precipitates ( $\sim 1.5 \cdot 10^7 \text{ cm}^{-3}$ ) remains unchanged in spite of increasing oxidation duration. It means that precipitates formation process is completed in the course of the crystal growth [84]. The formation of oxidation-induced stacking faults was registered by means of TEM after heat treatment at 1373 K in steam within 5.0 min, although grown-in precipitates could not be observed. Since oxidation-induced stacking faults occur on oxygen precipitates formed in the process of growth, OSF-ring parameters should depend on the growing conditions. Investigation of the growth rate effect on distribution of grown-in microdefects in silicon single crystals with a diameter of 150 mm showed that the OSF-ring is observed in crystals grown at a moderate growth rate (0.7...0.8 mm/min) and is absent in crystals grown at 0.4 mm/min and 1.1 mm/min [84]. The critical growth rate at which the OSF-ring appearance or disappearance is observed in the center of the growing crystal is due to thermal conditions on the crystallization front. A change in thermal conditions is accompanied by a change in OSF-ring diameter contraction rate as the growth rate decreases:

the lower the axial temperature gradient, the faster the diameter of the ring is reduced.

The process of oxygen microprecipitates formation (nuclei of oxidation-induced stacking faults) is considered as a function of free vacancies concentration: formation of vacancy clusters dominates at a high concentration of nonequilibrium vacancies (in the central part of the vacancy zone), with its decrease (at the edge of the zone) interaction of vacancies and oxygen atoms with formation oxide particles take place [81]. Thus, the OSF-ring is formed at the edge of the vacancy area, the outer boundary of the ring adjoins the defect-free zone [85, 86]. The OSF-ring is formed due to nonuniform distribution of the axial temperature gradient at the crystallization front along the growing crystal radius, resulting in uneven radial distribution of the residual intrinsic defects. The formation of the OSF-ring is closely related to the dependence of oxygen precipitation kinetics on the concentration of free vacancies [81].

The microdefects detected by selective etching are differently distributed inside and outside the OSF-ring; the nature and distribution of microdefects vary substantially with the crystal growth rate change. The following types of defects are observed inside the ring at moderate and high growth rates, depending on the investigation methods:

- typical cone-shaped etching patterns detected in a result of selective etching (flow pattern defects, FPD) [87];
- double or triple octahedral voids with linear dimensions of 0.1...0.3  $\mu\text{m}$  detected by the scattered IR radiation method (light scattering tomography defects, IR LSTD) [88];
- etch pits detected by selective etching, similar to FPD but not cone-shaped (Secco etch pits defects, SEPD) [87];
- single or double pyramid-shaped small pits with a diameter of 0.12...0.3  $\mu\text{m}$  and a depth of about 0.14  $\mu\text{m}$ , faceted with planes {111}, detected on the silicon wafer surface before and especially after washing in  $\text{NH}_4\text{OH}:\text{H}_2\text{O}_2:\text{H}_2\text{O}$  solution (crystal originated particles, COPs) [89];
- defects detected by optical interferometry (optical precipitate profiler defects, - OPPD) [90].

As it was illustrated in [90], the above listed defects are likely different forms of the same defect revealed by various methods: vacancy complexes formed inside the OSF-ring. The relationship between them can be expressed as follows:  $(\text{IR LSTD} = \text{COPs} = \text{OPPD}) = \text{FPD} + \text{SEPD}$ . Heat treatment at high temperatures in an oxidizing atmosphere result in